Chapter 2

Theory of Digital Holography

As discussed in Chapter 1, holography is a two-step process, involving (i) recording of hologram which uses the principle of interference and (ii) reconstruction of hologram based on the principle of diffraction [1, 2, 4, 69, 71]. In digital holography recording is done on pixilated digital sensors [69]. Reconstruction is done by numerical implementation of scalar diffraction integrals from which the whole field information of recorded object wavefront can be obtained [11, 70, 85, 86]. In this chapter, theory behind the digital recording and reconstruction process of holograms is detailed.

2.1 Recording of holograms

First stage of holography is recording of the interference pattern (hologram) which arises due to superposition of the object and the reference wavefront [2, 4, 69, 71]. This interference pattern contains the amplitude and phase information of the waves scattered from the object. Off-axis geometry is used in all the developed techniques and applications, discussed in this thesis. In such geometry, source beam is split into two and one of them passes through the object and another behaves as a reference beam, and then both beams are allowed to interfere at digital sensor (Fig.2.1).

Photo-detectors are quadratic in nature and can respond only to the absolute square of complex amplitude (intensity) distribution. Hence hologram pattern is recorded in form of spatially varying intensity distribution by recording medium [2, 4, 11, 17, 30, 69, 70, 71, 84, 85, 86, 87]. If the complex amplitude distributions of the object and reference wavefronts at the recording plane (hologram plane)

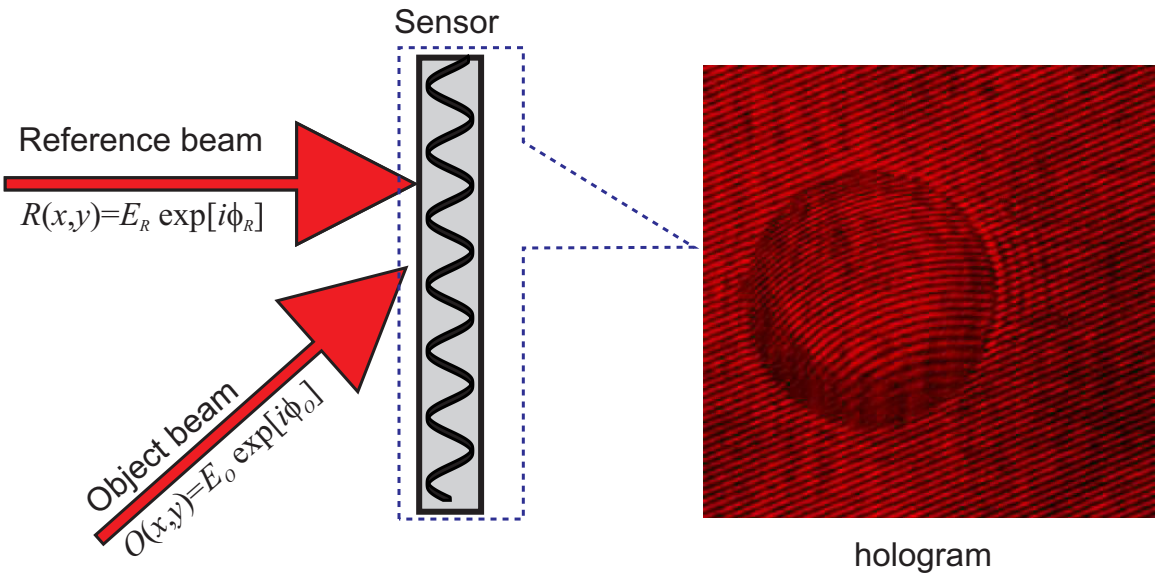

Figure 2.1: Formation of hologram due to superposition of the object and the reference wavefronts at the detector plane. Carrier fringes are modulated in the region where the object exists.

are $O(x,y) = E_O(x,y)exp[i\phi_O(x,y)]$ and $R(x,y) = E_R(x,y)exp[i\phi_R(x,y)]$ respectively (where E_O and E_R are their respective scalar amplitude distributions and ϕ_O and ϕ_R are their respective phase distributions), then the resulting intensity profile (hologram) sampled by the digital sensor can be written as [2, 4, 69, 71, 84]

$$\begin{aligned} I_H(x,y) &= |O+R|^2 = (O+R)(O+R)^* \\ &= (E_O exp[i\phi_O] + E_R exp[i\phi_R])(E_O^* exp[-i\phi_O] + E_R^* exp[-i\phi_R]) \end{aligned} \tag{2.1.1}$$

where * denotes the complex conjugation. Eqn.(2.1.1) can be simplified in terms of the intensities of the object and reference wavefronts

$$\begin{aligned} I_H(x,y) &= E_O E_O^* + E_R E_R^* + E_O E_R^* exp[i(\phi_O - \phi_R)] + E_R E_O^* exp[-i(\phi_O - \phi_R)] \\ &= I_O + I_R + E_O E_R^* exp[i(\phi_O - \phi_R)] + E_R E_O^* exp[-i(\phi_O - \phi_R)] \end{aligned} \tag{2.1.2}$$

where I_O and I_R are the intensity of the object and reference beam respectively. Collectively $(I_O + I_R)$ may be regarded as the background term and the cross terms can be regarded as the interference terms [4].

2.2 Reconstruction of holograms

Reconstruction of hologram is the second step in holography. In digital holography they are reconstructed numerically by illuminating them by an exact digital replica reference wave (Fig.2.2). This is numerically equivalent to multiplying Eqn.(2.1.2) by the reference wave [69, 70]

$$\begin{aligned} I_H(x,y)E_R exp[i\phi_R(x,y)] = (I_O + I_R)E_R exp[i\phi_R] \\ + I_R E_O exp[i\phi_O] + E_R E_R exp[2i\phi_R]E_O^* exp[-i\phi_O] \end{aligned} \tag{2.2.1}$$

In Eqn.(2.2.1) first term on the right hand side represents the reference wavefront passing through the hologram undiffracted (zero order) [70]. This term does not contain any information about the object. Second term contains the complex amplitude information of the object wave (at the hologram plane), which can be propagated to the image plane (where the object existed) to obtain information about the object. This is also called the virtual image (see Fig.1.4), since it is formed exactly at the position where the object existed and is an exact replica of the object. Last term on the right hand side produces a distorted real image of the object (see Fig.1.4). Since in the DHIM configurations discussed in this thesis, off-axis geometry is used, the three terms in Eqn.(2.2.1) will be separated at the hologram plane as well as at the image plane (Fig.2.2). From Eqn.(2.2.1), it can be seen that by illuminating the digital hologram by a numerical reference wave and propagating it to the image plane, the complex amplitude distribution of the object can be retrieved. Complex amplitude contains both the scalar amplitude (absorption/reflection profile) and phase information (thickness/depth profile) of the object.

As discussed above in digital holography the reconstruction of the object wave field (propagation of the scattered reference wavefront from hologram plane to image plane) is done numerically by simulating the diffraction process happening at the digitally recorded holograms when illuminated by the reference wave using scalar diffraction theory [69, 71]. The numerical reconstruction process can be based on the Fresnel-Kirchhoff diffraction integral employing Fresnel transform after Fresnel approximation [84, 89, 90]. Reconstruction can also be done employing the angular spectrum approach (ASP) to the scalar diffraction theory [69, 92, 93, 94, 95]. Each

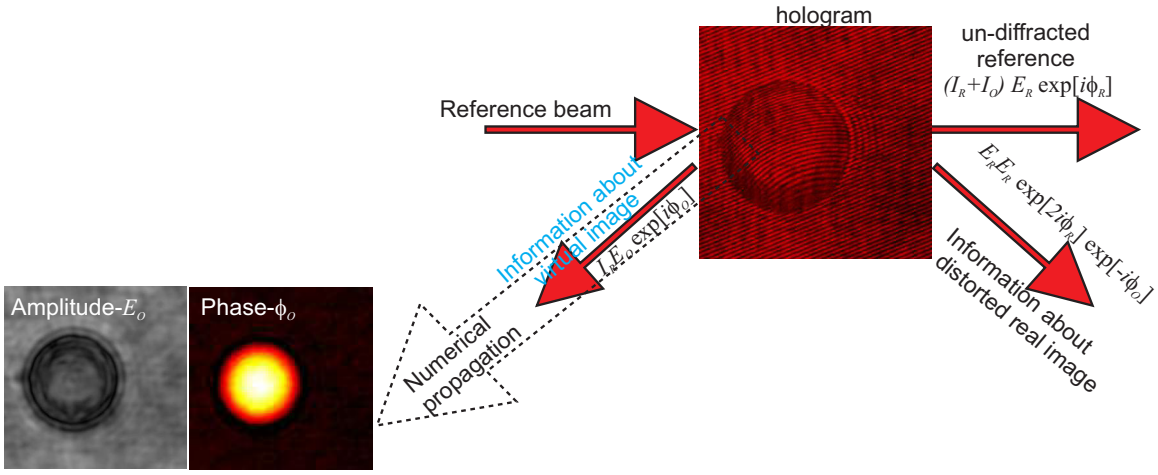

Figure 2.2: Digital hologram reconstruction. Reference wave gets scattered from the structures of the hologram. It is numerically propagated to the position where the object existed (virtual image).

of these approaches describes the scattering (diffraction) of the reconstructing wave from the structures of the hologram and the propagation of the scattered wavefront to the image plane. The numerical reconstruction process (scattering plus propagation) yields the object complex amplitude distribution, which contains information about the amplitude and phase of the object under investigation. For larger especially diffuse objects (objects kept large distance from the hologram), Fresnel-Kirchoff integral with Fresnel approximation (distance of propagation is much larger than size of the hologram - paraxial approximation) is the best approach to retrieve the object complex amplitude distribution [11, 70, 84, 85, 86, 89, 90].

In DHIM, the object (magnified image) is situated either at the detector plane or very near to the detector plane (Fig.2.3). It should be noted that the object information captured by the detector in this case is the magnified image of the micro-object as shown in Fig.2.3 [96]. It should be note that the propagation step can altogether be avoided by keeping the hologram plane (detector) at the image plane of the magnifying lens [36, 74, 75, 76, 83, 84]. So short distance propagations (or no propagation at all) is the requirement in the case of small transparent or phase objects imaged with DHIM. Angular spectrum approach describes the wavefront propagation over

short distances (no assumptions on the minimum distance of propagation - no paraxial approximation) compared to the size of the array (hologram). This is in contrast to Fresnel-Kirchoff integral which assumes propagation distances much larger than the hologram dimensions. So in the case of DHIM, angular spectrum propagation approach is ideal for image retrieval and also makes compact experimental setup possible. Another advantage of this approach is that, it can separate out the different diffracted components (un-diffracted reference, virtual object component, real object component) in the frequency domain (only the frequency information about the virtual/real object is propagated) and hence there will not be overlap between any of the three components in the reconstruction plane (image plane) [92].

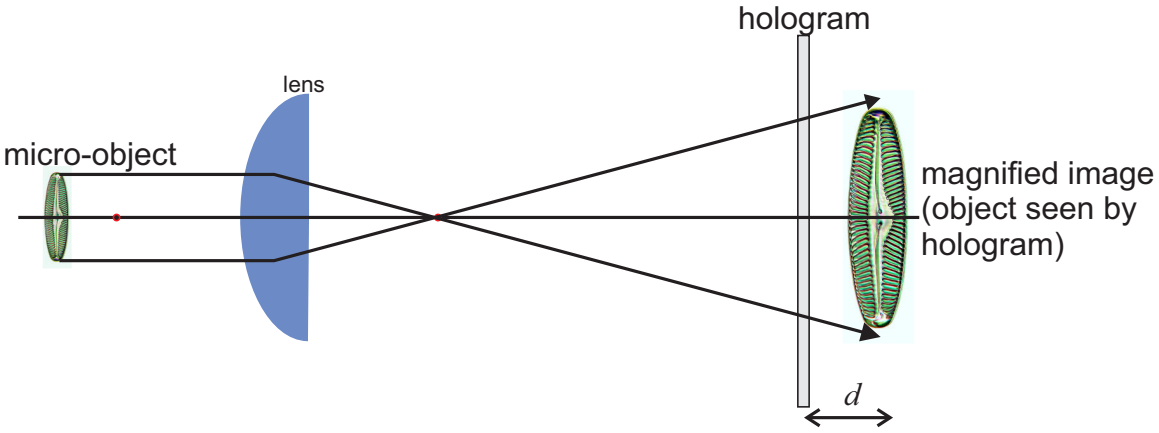

Figure 2.3: Position of the object (magnified image) and the hologram (detector) plane in DHIM. The object plane (magnified image plane) is situated either at the detector or very near to it.

2.3 Numerical propagation using Angular Spectrum approach

Waves scattering from an object can be considered in terms of plane wave components propagating at different directions (angles) [71] as shown in Fig.2.4. The angle of scattering of the object wavefront depends upon the spatial frequency components existing in the object and the complex amplitude of the wavefront at another parallel

plane can be computed by adding (integrating) the contributions due to these plane wave components [71].

For retrieval of object complex amplitude distribution using ASP approach (Fig.2.5), in the first step, digital holograms are illuminated by the reference wavefront giving rise to the complex amplitude at the hologram plane, which can be written as [30]

$$U(x, y, z = 0) = I_H(x, y)E_R exp[i\phi_R(x, y)] \tag{2.3.1}$$

In Eqn.(2.3.1), $z = 0$ is the hologram plane and U(x, y, $z = 0$) is the complex amplitude at the hologram plane due to illumination of the hologram by the reference wavefront. The aim of the numerical processing is to propagate this complex amplitude distribution to the plane, where the object (magnified image) existed (Fig.2.5).

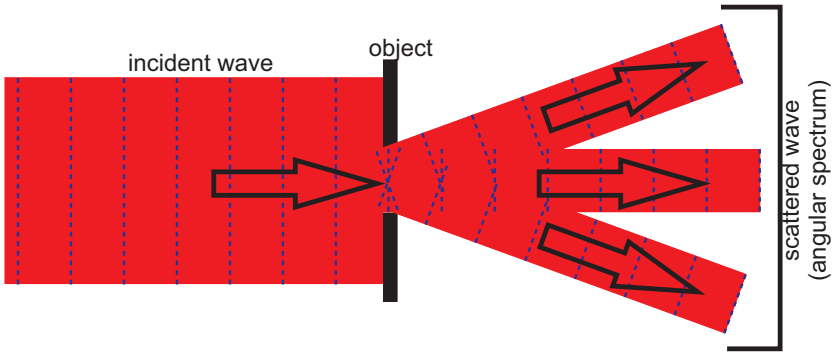

Figure 2.4: Scattered wavefront as a collection of plane waves travelling in different directions (angle). The scattering angle is decided by the spatial frequency of the object (smaller objects, higher spatial frequencies) scatter at higher angles. An object with sinusoidal intensity variation (like a hologram), will give rise to only three scattered components (only one frequency component).

Angular spectrum at $z = 0$ plane is obtained by Fourier transformation of Eqn.(2.3.1) and can be written as

$$\hat{U}(f_x, f_y; z = 0) = \int_{-\infty}^{\infty} \int U(x, y, z = 0)exp[i2\pi(f_x x + f_y y)]dxdy \tag{2.3.2}$$

In the above equation $(f_x, f_y; z = 0)$ is the Fourier transform at the hologram plane of the scattered reference wavefront, with f_x and f_y as the spatial frequencies in the

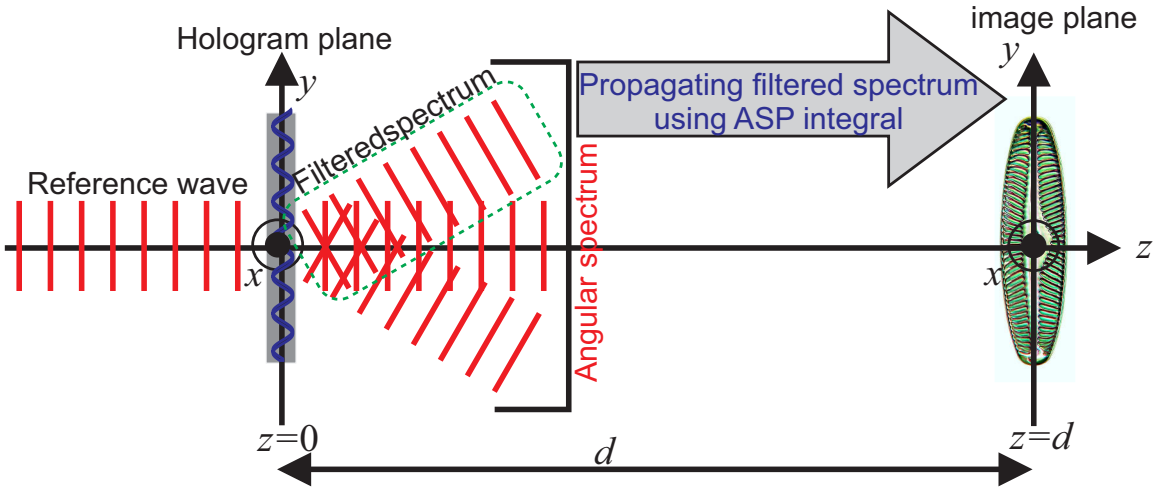

Figure 2.5: Numerical reconstruction of digital holograms using ASP approach. Reference wave illuminating the hologram generates the angular spectrum at the hologram plane (z=0), which is filtered (to obtain angular spectrum of object wavefront at the hologram plane) and then propagated to the image plane using free space propagation function.

x and y direction respectively. Fig.2.6b shows the angular spectrum of the hologram shown in Fig.2.6a. This is an off-axis hologram recorded with DHIM employing Mach-Zehnder geometry (geometry similar to that shown in Fig.1.7). A random linearly polarized He-Ne laser (λ=632.8nm, o/p power $<$ 2mW) was used as the source. An 8-bit CCD array with pixel pitch of 4.65μm was used for recording the holograms. Object was 20 μm diameter polystyrene microsphere (refractive index=1.58), immersed in oil (refractive index=1.518). A 40X, NA=0.65 microscope objective lens was used for magnification.

Filtering (using a circular band pass filter) is be applied to the resulting spectrum (Fig.2.6b) so that the unwanted terms, first and last term in Eqn.(2.2.1) can be removed. These terms corresponds to the un-diffracted reference wave and the distorted real object respectively. By this filtering, the spectrum corresponding to the object only can be obtained. Basically Fourier transform decomposes the complicated function into a series of simple complex functions. So the inverse Fourier transform of the filtered spectrum of Eqn.(2.3.2) provides the modified complex amplitude at $(x, y, z = 0)$ containing the information about the object only (Fig.2.6c). This can be

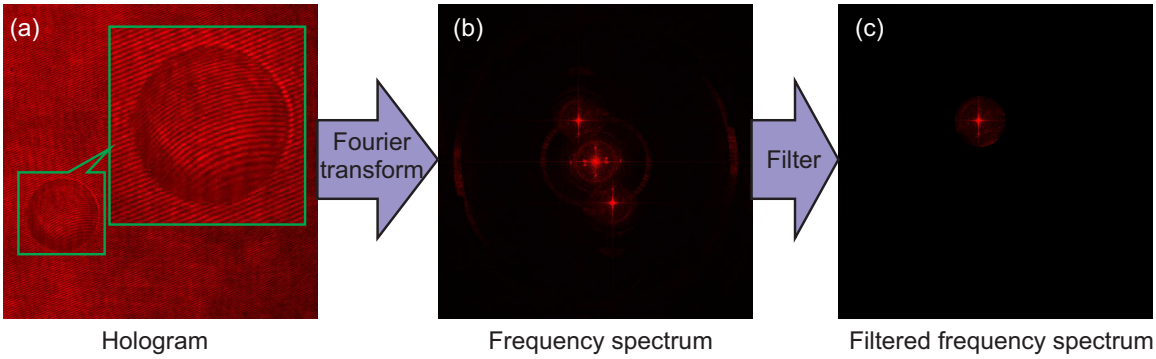

Figure 2.6: (a) Hologram illuminated by the reference wavefront. (b) Power spectrum of the hologram obtained after Fourier transform, where three components (un-diffracted reference, real object and virtual object) can be seen. (c) Filtered spectrum, which contains only the spatial frequencies corresponding to object alone. This is then propagated to the image plane.

written as [71, 92]

$$\bar{U}(x,y,z=0) = \iint_{-\infty}^{\infty} filt[\hat{U}(f_x,f_y;z=0)]exp[i2\pi(f_x x + f_y y)]df_x df_y \qquad (2.3.3)$$

where $\bar{U}(x,y,z=0)$ is the filtered (modified) complex amplitude distribution (containing only object information) and $filt[\hat{U}(f_x,f_y;z=0)]$, is the filtered angular spectrum of $U(x,y,z=0)$. If the complex amplitude at a plane parallel to the (x,y) plane but a distance z=d from the $(x,y,z=0)$ plane is known, then the angular spectrum at this plane can be written as [71]

$$\hat{U}(f_x,f_y;z=d) = \iint_{-\infty}^{\infty} U(x,y,z=d)exp[-i2\pi(f_x x + f_y y)]dxdy \qquad (2.3.4)$$

If the relationship between the angular spectrums at $(x,y,z=0)$ and $(x,y,z=d)$ can be determined, the effect of wave propagation on the angular spectrum can be determined. So the object complex amplitude distribution at $(x,y,z=d)$ can be written in terms of its angular spectrum [71]

$$U_o(x,y,z=d) = \iint_{-\infty}^{\infty} \hat{U}(f_x,f_y;z=d)exp[i2\pi(f_x x + f_y y)]df_x df_y \qquad (2.3.5)$$

This wave field should satisfy the Helmholtz equation, whose solution can be written in terms of the filtered spatial frequency distribution at the hologram plane

as [92]

$$\hat{U_o}(f_x, f_y; z = d) = filt[\hat{U}(f_x, f_y; z = 0)]exp[ik\sqrt{1 - \lambda^2 f_x^2 - \lambda^2 f_y^2}d] \tag{2.3.6}$$

The effect of propagation over a distance z=d is simply a change in the relative phases of the various components of the angular spectrum [71]. Each plane wave components travels at a different angle and hence travel different distances between the two parallel planes (hologram and image) producing phase delays. In Eqn.(2.3.6), λ is the vacuum wavelength of the light source that illuminates the hologram. Inverse Fourier transform of Eqn.(2.3.6) will yield the complex amplitude at $(x, y, z = d)$ as [92]

$$\begin{aligned} U_o(x, y; z = d) = \iint_{-\infty}^{\infty} \bar{U}(f_x, f_y; z = 0)exp\left[ik\sqrt{1 - \lambda^2 f_x^2 - \lambda^2 f_y^2}\ d\right] \\ \times exp[i2\pi(f_x x + f_y y)]df_x df_y \end{aligned} \tag{2.3.7}$$

The above relationship can be numerically implemented by first Fourier transforming the wave field at the hologram plane, filtering it and multiplying it with the free space propagation function (first exponential function in the above equation) and then taking its inverse Fourier transform. Eqn.(2.3.7) can then be written as [30, 92]

$$U_o(x, y; z = d) = \Im^{-1}\left\{filt[\Im\{U(x, y, z = 0)\}]exp\left[ik\sqrt{1 - \lambda^2 f_x^2 - \lambda^2 f_y^2}\ d\right]\right\} \tag{2.3.8}$$

In the numerical reconstructions of holograms recorded using DHIM discussed in this thesis Eqn.(2.3.8) is used to retrieve the object complex amplitude distribution. If the hologram plane (digital array) is at the image plane of the magnifying lens, then $d = 0$ and Eqn.(2.3.8) reduces just to Fourier fringe analysis [97].

2.4 Retrieval of intensity and phase of object wavefront

Complex amplitude at the image plane is numerically computed using Eqn.(2.3.8). The most important parameter in Quantitative phase imaging modality like DHIM is the phase of the object wavefront. Eqn.(2.3.8) can be used to retrieve the intensity

and phase information of the object. The intensity of the wavefront is equal to the absolute square of the complex amplitude and can be written as

$$I_o(x,y) = |U_o(x,y)|^2 \tag{2.4.1}$$

Fig.2.7 shows the object intensity distribution at the image plane obtained by numerical propagation in the case of the hologram shown in Fig.2.6a.

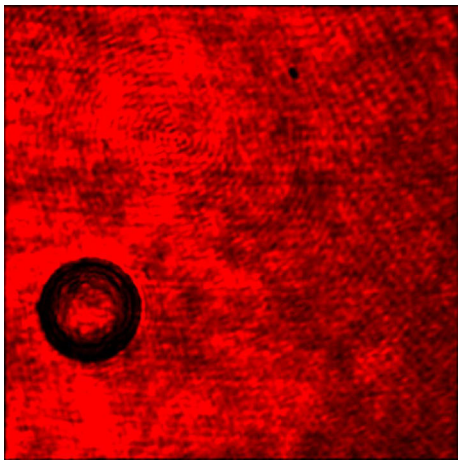

Figure 2.7: Retrieved intensity profile at the image plane for the hologram shown in Fig.2.6a

Phase of the object wavefront is calculated from the angle the complex amplitude makes with the Real axis

$$\phi_o(x,y) = arctan\frac{Im[U_o(x,y)]}{Re[U_o(x,y)]} \tag{2.4.2}$$

For each hologram of the object (object hologram) a background hologram (Fig.2.8b), without the object in the field of view (only the medium surrounding the object will be in the field of view) and by keeping all the other parameters same, is also recorded. This hologram is also reconstructed using Eqn.(2.3.8) and the phase is retrieved

$$\phi_B(x,y) = arctan\frac{Im[U_B(x,y)]}{Re[U_B(x,y)]} \tag{2.4.3}$$

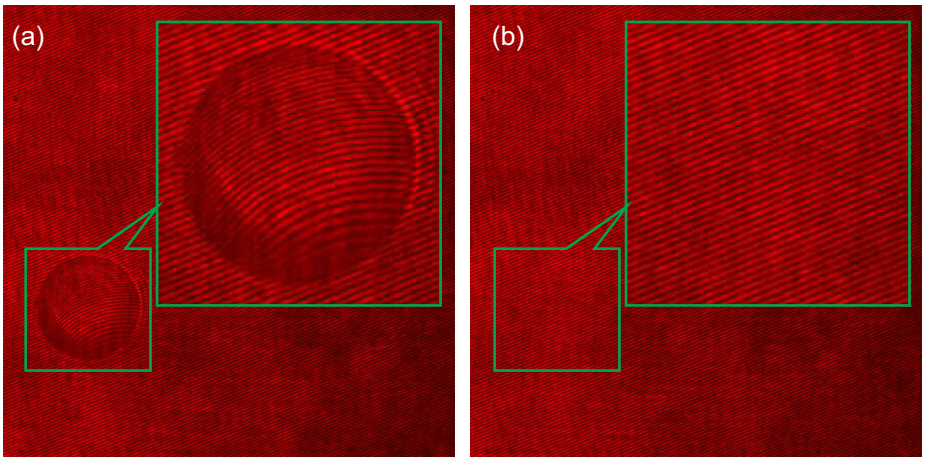

Figure 2.8: (a) Object hologram of the 20 μm diameter polystyrene sphere immersed in oil. (b) Background hologram of the background (oil). Inset in both the images shows the same area in the field of view.

2.5 Phase difference and object thickness

Phase difference (interference phase) is computed directly by subtracting the background phase distribution from the object phase distribution [69].

$$\begin{aligned} \Delta\phi(x,y) &= \phi_o(x,y) - \phi_B(x,y) \qquad if \phi_o > \phi_B \\ &= \phi_o(x,y) - \phi_B(x,y) + 2\pi \qquad if \phi_B > \phi_o \end{aligned} \tag{2.5.1}$$

This phase subtraction nullifies the aberrations due to optical elements, as the parameters other than the object remained same between the exposures. This brings out the phase distribution due to the object alone, negating the phase due to aberrations [30, 84]. Fig.2.9 shows the process of phase subtraction, which brings out the object phase information after compensating for the phase due to aberrations in the system. Phase shown in Fig.2.9c is wrapped (phase variation between 0 and 2 π). This needs to be unwrapped to convert it into continuous phase distribution before using it in thickness profiling of the object. Fig.2.10 shows the unwrapped phase distribution applying Goldstein branch cut unwrapping method.

The phase difference acquired by the object beam that passes through the object is given by Eqn.(2.5.1). This phase difference is proportional to both the refractive

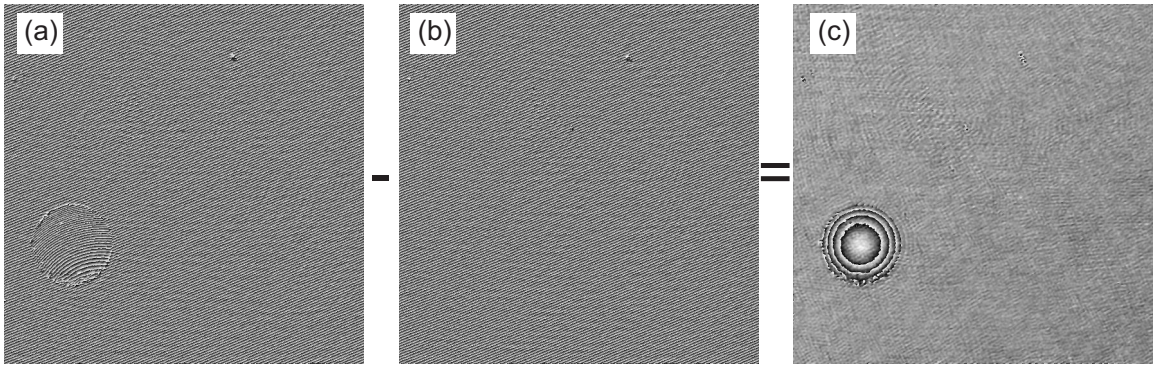

Figure 2.9: (a) Object phase distribution (object is a 20μm diameter polystyrene sphere immersed in oil). (b) Background (oil) phase distribution. (c) Phase difference.

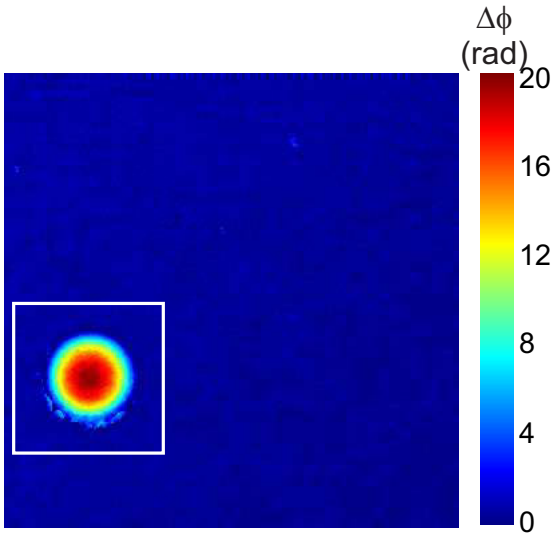

Figure 2.10: Continuous phase distribution for the wrapped phase distribution shown in Fig.2.9c.

index difference between the object and the surrounding medium (background) and the thickness of the object itself [30, 36, 83, 84].

$$\Delta\phi(x,y) = \frac{2\pi}{\lambda}(n_o - n_B)L(x,y) \tag{2.5.2}$$

In Eqn.(2.5.2), n_O and n_B are the constant average refractive indices of the object and the background respectively and L is the spatially varying thickness of the object. Eqn.(2.5.2) can also be expressed as

$$\Delta\phi(x,y) = \frac{2\pi}{\lambda}\Delta nL(x,y) \tag{2.5.3}$$

In Eqn.(2.5.3), Δn is the refractive index difference between the object and the background. The spatially varying optical path length ($OPL = \Delta n \times L$) distribution is either due to a spatial variation in refractive index or the or due to a spatially varying thickness. In the cells investigated, the spatial variation in OPL is bought about by spatial variation in thickness rather than refractive index, which could be assumed to be a constant. If the refractive index values are known, then Eqn.(2.5.3) can be used to construct the thickness distribution (3D image) of the object. Fig.2.11 shows the 3D rendering of the thickness profile of the 20μm diameter polystyrene microsphere constructed from the continuous phase distribution shown in Fig.2.10. In the thickness reconstructions, $n_O = 1.58$ and $n_B = 1.518$ were used.

Fig.2.11 summarizes the quantitative phase imaging by numerical reconstruction of digital holograms. Object and background holograms are reconstructed by the numerical implementation of Eqn.(2.3.8). Their reconstructed complex amplitude distributions at the image plane are used to calculate the object and background phases using Eqn.(2.4.2) and Eqn.(2.4.3) respectively. Then the phase difference is computed to nullify the aberrations and to bring out the object phase distribution by the use of Eqn.(2.5.1). Continuous phase difference after phase unwrapping is shown in Fig.2.11a. The obtained phase difference along with the refractive index values are plugged into Eqn.(2.5.3), to construct the object thickness profiles shown in Fig.2.11b and Fig.2.11c. It should also be noted that by changing the value of d in Eqn.(2.3.8) information at different object planes can be obtained (even though path integrated), which might provide important object information, which might be

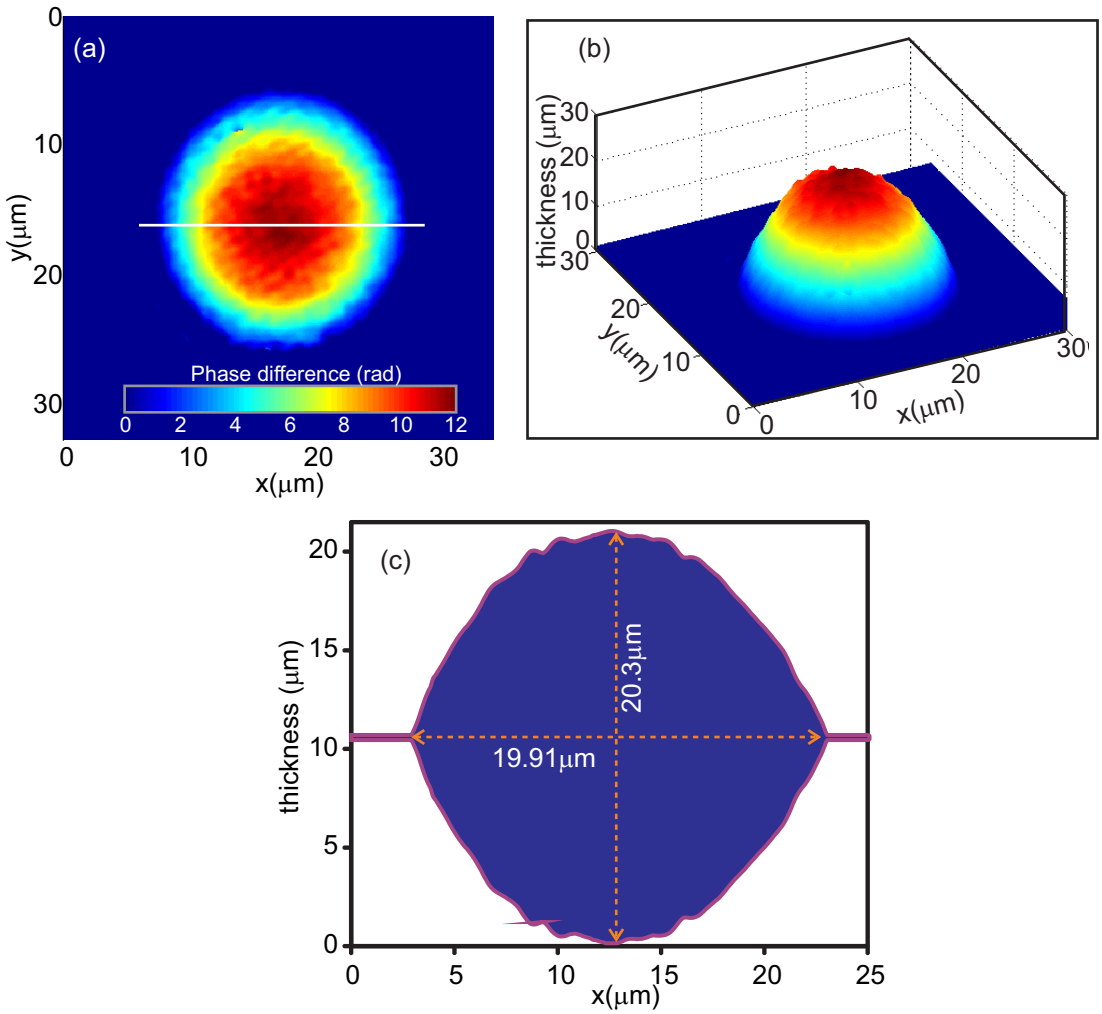

Figure 2.11: Quantitative phase reconstruction from digital holograms. (a) Continuous phase difference obtained in the case of 20μm diameter polystyrene micro-spheres. This is the region of interest shown by the rectangular area in Fig.2.10. (b) Thickness distribution of the micro-sphere obtained by plugging in the refractive index values in Eqn.(2.5.3). (c) Cross sectional thickness profile of the micro-sphere along the solid line shown in Fig.2.11a.

useful in its identification [36].

For the DHIM techniques discussed in this thesis, numerical reconstructions of holograms are achieved by the use of angular spectrum propagation integral given by Eqn.(2.3.8). The resulting phase images are used to compute the object thickness as well as its time evolution. Also various static and dynamic parameters for the object under investigation are extracted from the reconstructed thickness profiles. In many cases, especially in the case of object identification and comparison, it is not necessary to have the refractive index values of the cell and the background medium. Optical path length profiles are sufficient to quantify, compare and identify object using DHIM [34].